Polymers & biopolymers

Effect of dehydration method on the micro- and nanomorphological properties of bacterial cellulose produced by *Medusomyces gisevii* on different substrates

Natalia Pogorelova[1], Evgeniy Rogachev[2], Nuraly Akimbekov[3], and Ilya Digel[4,*]

[1] *Omsk State Agrarian University, Omsk, Russian Federation 644008*

[2] *Omsk State Technical University, Omsk, Russian Federation 6440050*

[3] *Al-Farabi Kazakh National University, Almaty, Kazakhstan*

[4] *Institute for Bioengineering, FH Aachen University of Applied Sciences, 52428 Jülich, Germany*

ABSTRACT

Many important properties of bacterial cellulose (BC), such as moisture absorption capacity, elasticity and tensile strength, largely depend on its structure. This paper presents a study on the effect of the drying method on BC films produced by *Medusomyces gisevii* using two different procedures: room temperature drying (RT, (24 ± 2 °C, humidity 65 ± 1%, dried until a constant weight was reached) and freeze-drying (FD, treated at − 75 °C for 48 h). BC was synthesized using one of two different carbon sources—either glucose or sucrose. Structural differences in the obtained BC films were evaluated using atomic force microscopy (AFM), scanning electron microscopy (SEM), and X-ray diffraction. Macroscopically, the RT samples appeared semi-transparent and smooth, whereas the FD group exhibited an opaque white color and sponge-like structure. SEM examination showed denser packing of fibrils in FD samples while RT-samples displayed smaller average fiber diameter, lower surface roughness and less porosity. AFM confirmed the SEM observations and showed that the FD material exhibited a more branched structure and a higher surface roughness. The samples cultivated in a glucose-containing nutrient medium, generally displayed a straight and ordered shape of fibrils compared to the sucrose-derived BC, characterized by a rougher and wavier structure. The BC films dried under different conditions showed distinctly different crystallinity degrees, whereas the carbon source in the culture medium was found to have a relatively small effect on the BC crystallinity.
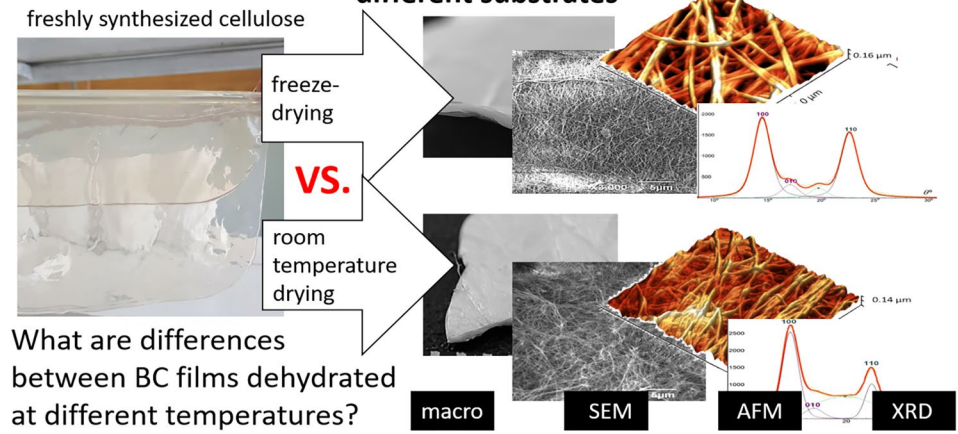

GRAPHICAL ABSTRACT

Effect of dehydration method on the micro- and nanomorphological properties of bacterial cellulose produced by *Medusomyces gisevii* on different substrates

Introduction

Bacterial cellulose (BC) is a linear extracellular polysaccharide composed of glucose and glucose-6-phosphoethanolamine units, synthesized in fairly large quantities by representatives of the genera *Gluconacetobacter*, *Acetobacter*, *Azotobacter*, *Pseudomonas*, *Alcaligenes*, *Agrobacterium*, *Sarcina* and *Rhizobium* [15]. Furthermore, BC is a minor but common component of biofilms produced by many Enterobacteriaceae [26].

In BC-synthetizing bacteria, it presumably contributes to many vital functions, including the integrity of the bacterial cell envelope, mechanical, chemical and physiological protection, cell adhesion, and biofilm stability [22]. Due to its porous three-dimensional fibrillar crystalline structure, resulting in high water-holding capacity, high elasticity and stiffness, as well as excellent biocompatibility and high chemical homogeneity, BC has been increasingly used in many fields, including numerous applications in biomedical engineering [4, 19].

Unfortunately, more intensive (and extensive) use of BC is still hindered by sample-to-sample variability of its properties and potential quality deterioration, which becomes especially pronounced with production scaling up or upon varying technological process parameters [21]. Indeed, a number of studies conducted by us and other authors in recent years have already shown the relationship between the structure of the polymer and the type of cultivation (static or dynamic mode), used strain of bacteria, composition of the nutrient medium, and many other factors [2, 3, 7, 19]

In its natural form, bacterial cellulose represents a hydrogel, containing just 1.5–2.0% dry matter. However, for many practical applications, most BC water needs to be removed to achieve better mechanical performance and to increase chemical stability. Drying also makes BC materials more portable and convenient to use. For this reason, the majority of existing BC production methods include drying/dehydration steps. Dehydration of BC can be achieved by different approaches, including freeze-drying (lyophilization), a combination of thermo-mechanical factors (e.g. hot pressing), or simply by "passive" drying at room temperature. In 1999 Madihally et al. proposed the process of freeze-drying membranes as a possible way to maintain a reasonable primary BC structure, and here we will follow this approach to obtain cellulose membranes in addition to the conventional process drying by simple evaporation of the solvent [16].

The drying method can be crucial to the structure, performance, and application of BC films. In 2006, Clasen et al. [5] showed that freeze-drying resulted in a significant increase in gas permeability and swelling degree of BC films produced by *Gluconacetobacter xylinus*, compared to the evaporation-dried BC samples. Five years later, Zhang et al. [29] demonstrated that the choice of a drying method and its parameters may significantly affect the properties of the final BC

product. They found that the mechanical properties of BC films dried by hot air were significantly better than those of samples dried in a vacuum freeze-drying machine. However, some later studies suggested that lower drying temperatures can improve the deformation characteristics of dehydrated BC films [8]. In the last decade, scientific and practical interest in the dehydration of cellulose gel films was focused mainly on studying physical/mechanical characteristics, while the dependence of micro- and nanomorphological structure and crystallinity on the chosen drying protocol has yet to be scrutinized.

The several existing studies devoted to nanomorphological effects related to the drying process vary significantly in their interpretation and evaluation of the influence of dehydration process parameters (temperature, duration and other) on the crystallinity index of cellulose. Vasconcellos and Farinas reported that oven-dried BC exhibited a dense structure with collapsed fibers in contrast to the loose and porous surface of the freeze-dried material [27]. In their study, the thermal stability of the BC films also depended on the drying method, being 6 °C higher in the freeze-dried samples, although differently dried BC films displayed similar crystallinity degrees.

Later, Illa et al. pointed out that oven-dried BC possessed slightly higher crystallinity and lower fiber diameter as compared to freeze-dried BC [12]. They also reported larger crystallite size and pore size of the lyophilized BC. In contrast, when comparing BC samples dehydrated at 25 °C, 50 °C, and 100 °C, Rosyida et al. found no differences in their surface morphology. At the same time, they argued that higher drying temperatures tend to cause higher BC fragility due to higher crystallinity [23]. Interestingly, these findings do not quite coincide with the results published by Mohammad et al., who pointed out that high-temperature dehydration of BC lowered its thermal stability and reduced the crystallinity index by ± 5.0% compared to freeze-drying [17].

We think that dehydration is not only an essential downstream processing step in BC production but also a potentially useful tool for adjusting and tuning the BC properties for a given application. Nevertheless, despite the aforementioned studies, systematic data on the effect of the drying method on the BC surface properties and crystalline structure are still deficient. Here, we are presenting an experimental case study examining the relationship between the drying method and the composition of the culture medium on one side

and the nanostructure of BC on the other side. Our hypothesis was that BC films dehydrated at different temperatures and with different speed will not only have different appearance and mechanical properties but also will differ on the nanoscale—in particular, in their nano- and microfiber alignment patterns and in their crystallinity degree. For better assessment and analysis of the fibrillar structure of bacterial cellulose films dehydrated under different conditions, in this work we have collected and compared data obtained from atomic force microscopy (AFM), scanning electron microscopy (SEM), and X-ray diffraction (XRD).

Materials and methods

Culture medium composition and biosynthetic process

Symbiotic microbial consortium *Medusomyces gisevii*, also known as the "Kombucha fungus" was acquired from the Scientific Center Kurchatov Institute—Research Institute for Genetics and Selection of Industrial Microorganisms (Russia). This steady microbial community is composed of 15–30 genera represented by yeasts (predominantly *Zygosaccharomyces* sp.) and the acetic acid bacteria (mainly *Gluconacetobacter xylinus*, conventionally known as *Acetobacter xylinum*). More exact species composition of the Kombucha culture is detailed elsewhere [13, 14].

Two variants of culture medium differing in their principal carbon source were used for cellulose biosynthesis by *Medusomyces*. The culture medium consisted either of 7.5% glucose, or of 7.5% sucrose (Sigma-Aldrich Co.) dissolved in 0.4% extract of plain green tea (Woodbury Sugar Shed Co. USA). The tea solution was prepared by infusing 4 g of dry green tea in 1 L of hot (80 °C) tap water for 15 min, resulting in approx. 1.21 g·L^{-1} green tea extractives in the medium. This medium is considered "selective" for *Medusomyces*, so that cultivation can be carried out under non-sterile conditions.

The BC biosynthesis by *Medusomyces* was carried out under batch cultivation conditions within cuboid polypropylene tanks (15 cm height × 17 cm width × 10 cm length) at 25 ± 2 °C. The medium was inoculated with a suspension of *Medusomyces* biomass previously adapted for 7 days for the corresponding carbon source. The initial volume of the culture medium in the tank was 1.5 L, and the initial ratio of

the inoculum to the culture medium was adjusted to 1:3 (v/v). The active (titratable) acidity was followed daily but never adjusted during cultivation. The BC was formed as a swollen gel pellicle (film) at the air–water interface, and its thickness correlated with cultivation time.

Cellulose purification and drying

BC pellicles were collected and examined on 8th day of cultivation. After the cultivation period, the content in the tank was vigorously stirred for 10–15 min to reduce the number of attached microbial cells. BC pellicles at the air/liquid interface were manually separated from the culture liquid, gently squeezed out, and washed with deionized water until neutral pH values were reached. Each resulting gel sample was collected and analyzed in triplicate (i.e., from three different culture tanks).

The rinsed BC material was incubated in the equal volume of 0.1 M NaOH at 80 °C for 90 min to remove the remaining microbial cells. This step was repeated four times until a (perceptibly) colorless transparent BC pellicle was obtained. The resulting BC pellicle was rinsed with deionized water until neutral pH values were reached (7.0 ± 0.6). The wet weight of the cellulose gel pellicles was measured using a laboratory balance.

After washing, dehydration of the cellulose samples was carried out in two ways: (a) BC was pre-frozen at -70 °C for 6 h and then freeze-dried (lyophilized) at -75 °C for 48 h using a pilot-scale shelf freeze-dryer Jaba-Lyoph-Pride (ilshinBioBase, Dongduchon, South Korea), and (b) BC was allowed to dry under room conditions (temperature 24 ± 2 °C, humidity $65 \pm 1\%$, until constant weight. Further in the text, the first and the second methods are referred to as RT-method (room temperature) and FD-method (freeze-dried), respectively. After dehydration, the BC samples were stored at room temperature in plastic containers until further tests.

Characterization of bacterial cellulose

The RT- or FD- samples synthesized on glucose or sucrose media for 8 days were examined and compared in terms of their macro-, micro- and nanomorphological features.

Scanning electron microscopy (SEM)

The primary examination of the spatial orientation of BC macrofibrils was carried out by SEM. For each experimental variant, at least three specimens previously cut into 2×2 mm pieces using a sharp blade were examined using a scanning electron microscope JCM 5700 (JEOL Ltd. Japan). Since the studied samples of BC are dielectrics, low accelerating voltages were used, not exceeding 5 kV.

SEM images were taken in the plane perpendicular to the BC film surface from at least three different randomly selected positions of three different BC samples, using magnifications ranging from $\times 500$ to $\times 20000$. Quantitative data related to the size of inclusions, average pore size and fiber alignments were obtained using the JCM 5700 image analysis software tools by taking the mean value of 20 individual measurements and the standard deviation for each measured parameter.

Atomic force microscopy (AFM)

Information about sample surface topology and fibrillar structure was obtained using the atomic force microscope NTEGRA Prima (NT-MDT Spectrum Instruments, Russia) operated in a semi-contact mode. The scanning was performed in the air by HA-NC Etalon Series cantilever with a characteristic stiffness of 3.5 N/m. Amplitude and a phase of cantilever fluctuations were detected using an optical sensor.

Together with the "height" signal, allowing the investigation of the sample topography in three space coordinates, the "mag" signal was registered for better visualization of fine surface irregularities. Furthermore, the "mag" mode allows the detection of minor surface inhomogeneities, as it simulates the constant height mode, revealing the deviation of the probe when moving between adjacent surface points. The obtained signal was measured as a change in the photocurrent (pA) between the upper and lower sections of the optical sensor. AFM image processing and analysis were performed using the Gwyddion software developed by Nečas and Klapetek [18] and distributed under the GNU GPL license. Quantitative measurements of the pore size, fiber length, and diameter were done on the obtained images using NTEGRA image software tools. Average values and standard

deviations were calculated from 20 individual measurements for each parameter.

X-ray diffraction (XRD)

XRD measurements to assess the supramolecular structure of bacterial cellulose were performed on a diffractometer XRD-7000 (Shimadzu, Japan) with monochromated $Cu_{K\alpha}$ radiation in the θ–2θ mode. The diffractograms were recorded between 2θ angles of 10° and 30°. The applied tube voltage was 40 kV, current 40 mA. Deflection, scattering and receiving slits were set to 1°, 1°, and 0.15 mm, respectively. Data analysis was carried out in reflection geometry.

A common problem in analyzing diffractograms is the choice of the peak shape function. In this work, to approximate the line contours on the X-ray pattern, the pseudo-Voigt function pV(x) was used, which has the form:

$$pV(x) = \eta L(x) + (1 - \eta)G(x) \qquad (1)$$

where the weighting parameter η determines the ratio of the Lorentzian (L) and Gaussian (G) fitting components [1, 6]. Data processing and pseudo-Voigt fitting of the XRD peaks was performed in Fityk software (https://fityk.nieto.pl/) under the assumption that the reflection of the (100), (010), and (110) crystal planes of the cellulose corresponds to 14.4°, 16.8°, and 22.6° of 2θ respectively [28]. Therefore, the amorphous area was considered to be centered at approximately 18.5°. The obtained integral intensities were used to calculate the crystallinity index (CI) by the Ruland-Vonk method [2].

This method also allows to derive BC crystallite sizes (SC) from the ratio of the area of the crystalline phase to the total area under the diffraction curve, which includes scattering by the amorphous and crystalline phases. The initial stage of the calculation consisted in determining the position of the maximum and fitting the peaks of the crystalline component. Next, the numerical data on the areas of the crystalline and amorphous phases, the width of the reflections at half maximum, and the diffraction angles were refined and analyzed using the Fityk program. The background correction was performed by subtracting the baseline values connecting the horizontal sections in the lower part of the spectrum. The size of the coherent scattering region also was calculated from the X-ray data. This parameter characterizes the area in

the material in which the three-dimensional periodicity of the arrangement of atoms is preserved.

The lattice (inter-atomic) spacing d was determined using the classical Bragg equation for each diffraction angle:

$$D = \lambda/2\sin\theta \qquad (2)$$

An increase in the half-width of the peak in the X-ray diffraction pattern (parameter D_{fwhm} is the width of the X-ray peak at half its height) indicates a decrease in the size of crystallites. This information was important for understanding the sizes of ordered regions in the material, which, along with the proportion of these regions (the CI parameter), helps to understand the BC nanostructure more comprehensively [9, 10, 25].

Results and discussion

BC macrostructure and appearance

BC samples produced on glucose and sucrose were subjected to two different drying methods: room temperature drying (RT) or freeze drying (FD). Figure 1 shows the appearance of representative samples at the end of these drying processes. The pictures where taken by using a mobile phone camera with optical (× 2) zoom.

It can be seen that similar to the previously published studies [17, 27], samples derived by different drying protocols looked macroscopically different—while the RT-films were semi-translucent, colorless, and smooth, the FD samples appeared opaque, whitish and exhibited sponge-like structure.

Visual examination revealed also a more condensed structure of the RT material. This might be caused by a rearrangement of BC macrofibrils in the RT-films due to the degradation of the porous network structure and the formation of a more densely arranged bundled muscular structures in the RT films. The possible underlining effects (as pointed by Clasen et al.) are the decrease of the fibrils volume and their aggregation during thermal dehydration (RT) which presumably lead to a decrease in the surface area of BC samples (observed as "shrinkage" of BC samples by 10–20%) [5].

The FD BC films were typically 700–900 μm thick; they showed high porosity and high fragility. The thickness of the RT-dehydrated films was

Figure 1 The appearance of the dehydrated BC gel film samples synthesized on glucose (**a** and **c**) and sucrose (**b** and **d**). The two upper pictures (**a** and **b**) show the RT samples after drying at 24 °C, and the lower pictures (**c** and **d**) represent the FD samples dehydrated by freeze-drying. All photos were taken using ×2 optical zoom.
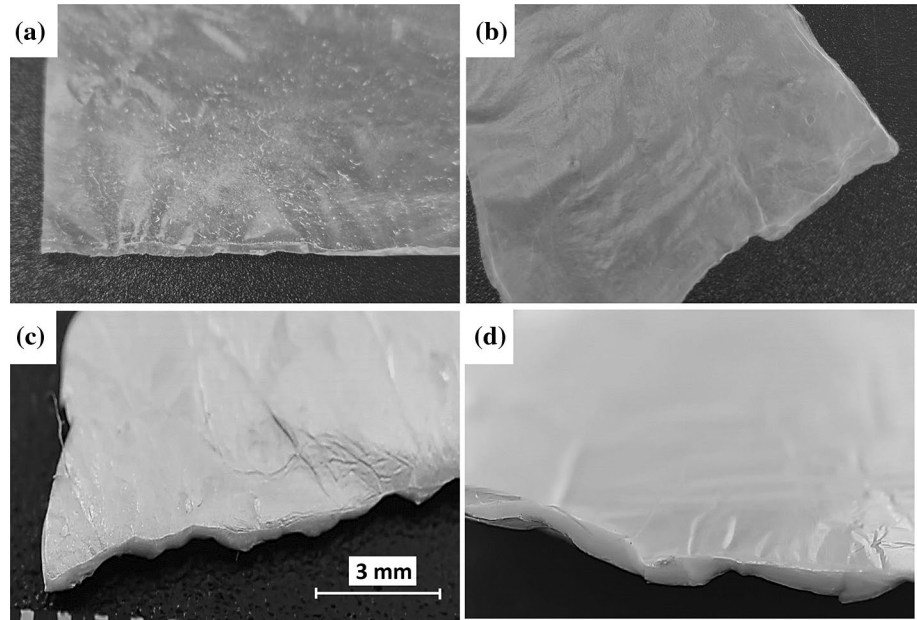
significantly less: between 80 µm and 110 µm. In comparison with FD samples, they were significantly more flexible. BC samples synthesized on glucose and sucrose did not differ from each other in terms of their thickness and appearance. We assume that slow (vs. fast) removal of water promotes irreversible aggregation of polymer chains, which results in permanent reduction in the elasticity of the RT samples, persisting even after later rehydration of the films. This is also reflected in the lower swelling capacity of the RT membrane compared to hydrated FD samples (data not shown).

It has already been reported that the mechanical strength and permeability of bacterial cellulose membranes are sensitive to processing after actual synthesis. Seifert et al. found that the swelling ability of a bacterial cellulose membrane depends on the subsequent drying process and that different swelling ratios are observed for re-swelling membranes [24]. They also proposed to modify the drying membrane by adding linear polymers.

BC microstructure and surface topology

In order to investigate the microstructure of the samples, they were examined using a scanning electron microscope. SEM-micrographs of the surface of samples grown in glucose media, and then subjected to different drying protocols are shown in Fig. 2a.

Similarly to the previously published studies, all BC films showed a hierarchical structure with pores of different sizes from macro to micro scale [17, 27, 29]. A change of the network structure of the bacterial cellulose by the different drying processes is already visible with SEM images. As shown in Fig. 2, the FD membrane possesses thinner fibers than the RT membrane.

The surfaces of both the RT- and FD samples often displayed globular inclusions 0.5–1.5 µm in diameter, presumably representing fragments of destroyed bacterial cells (Fig. 2, yellow arrow).

Comparison between glucose-derived BC samples dried by different methods revealed noticeably denser microfiber interweaving in the RT-group. A distinct feature of the freeze-dried samples was the presence of straight fibers reaching lengths of 50 ± 12 µm. The overall fiber packaging was not tight, with a rather chaotic plexus. These results are in good agreement with those by Zhang et al. [29], who reported that freeze-drying leads to less entanglement between fibrils and preserves the volume of cavities inside the BC films.

Likewise, in the sucrose-grown variants, a noticeable feature of the freeze-dried BC was its obviously higher porosity, while the fibers of the RT cellulose revealed a denser packing and the presence of numerous folds on the surface (Fig. 2b, left and right). Without regard to the differences caused by

Figure 2 SEM images of the surface of BC samples grown on glucose (**a**, upper row) and sucrose (**b**, lower row), FD (left) and RT (right). Yellow arrow: a globular inclusion (presumably fragments of destroyed microbial cells).
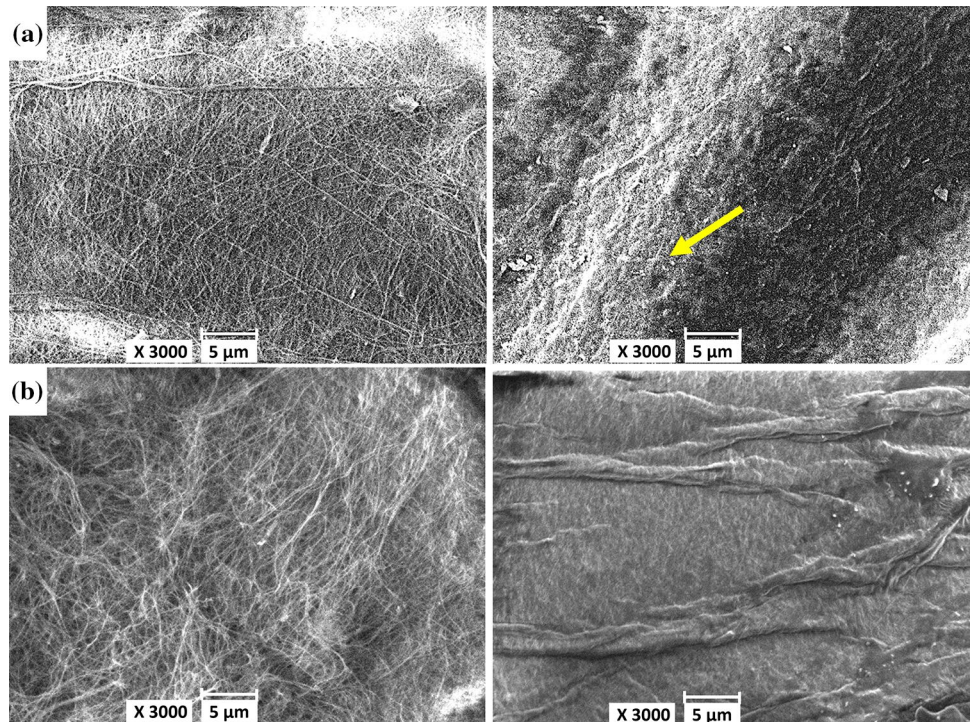

the applied drying procedure, the surface of samples synthesized on sucrose was more branched, dense, and heterogeneous. The structure of glucose-derived BC was found to be less entangled and less randomly intertwined.

The AFM-view of surface nanostructure of the BC samples synthesized on glucose medium and dried by different methods is shown in Fig. 3.

The morphology of the BC samples synthesized on glucose and then lyophilized (FD), showed a highly

Figure 3 AFM images of BC synthesized from glucose after FD (left) and after RT drying (right). The upper photos demonstrate the roughness of the sample according to the given pseudo-color scales. The pA values represent the photo-current measured. The lower row shows 3D-reconstructions of the obtained photos after converting pA units into height/roughness data.
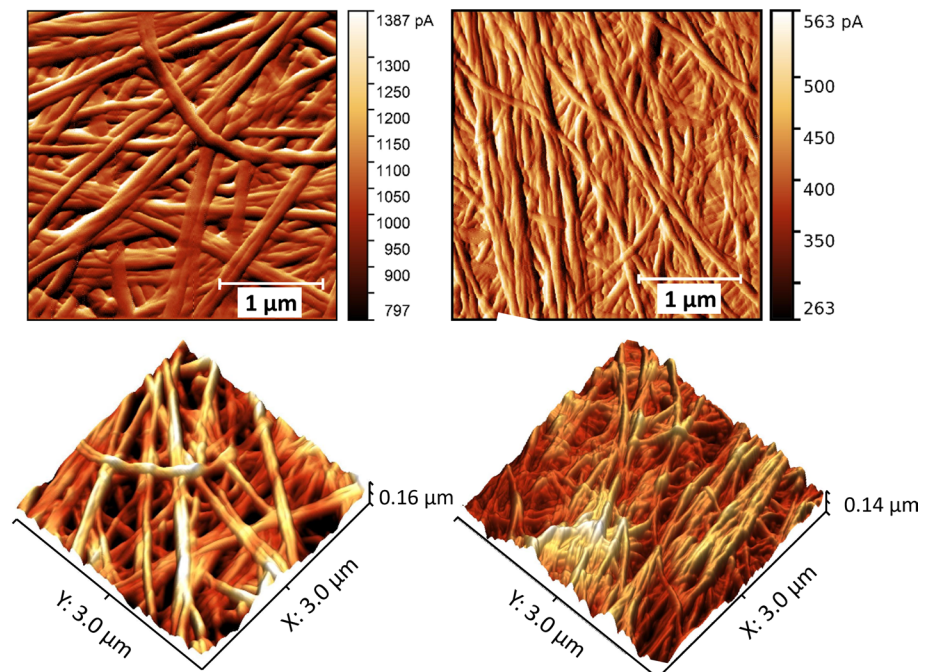
branched, porous structure with an average roughness of 195 nm (Fig. 3, left). Fibrils in the FD were randomly intertwined, however often displayed shapes resembling straight lines packed in parallel pairs. To obtain more accurate data on the fibril width, a series of additional scans was performed. The average width of fibers in the obtained surface profiles was close to 100 ± 15 nm.

Under conditions of room-temperature dehydration, BC material attained a denser packing of fibers (Fig. 3, right), which was accompanied by a significantly more uniform surface, with typical roughness not exceeding 81 nm. The length of fibers usually remained around 30 ± 7 μm. However, the fibers are intertwined more randomly, exhibiting multiple bends. A more detailed surface profile analysis showed that the average width was close to 55 nm, which was about 45% less compared to the FD group. Similar effects of lyophilization on material roughness and porosity were previously pointed out by Clasen et al. [5], who attributed the increase in the number of networks meshes and resulting higher roughness to the partial aggregation of free polymer strands during freeze-drying.

In our previous study, we investigated the influence of the carbon source and its concentration in the culture medium on the properties of the synthesized BC [7]. In BC-producing microorganisms, cellulose synthesis is accomplished by a multi-component membrane cellulose synthase complex which catalyzes the assembly of activated UDP-glucose units into a linear β-1,4-glucan chain (Acheson et al. 2019, Römling and Galperin 2015). The performance of this synthesizing machinery may be affected by the structure of the available substrate (carbohydrate). We found that the surface of samples synthesized on sucrose, tended to be more branched and heterogeneous. Compared to the glucose-derived variants, it also displayed slightly smaller pores (up to 0.2 μm in diameter), and had overall higher roughness [7]. Thus, it was interesting to examine to what if the BC films synthesized on sucrose would react to the drying conditions differently than those produced on the glucose substrate. The results are presented in Fig. 4.

Distinguishing features of the FD cellulose (Fig. 4, left) synthesized on sucrose were its wavy and branched surface with numerous bending fibers, as well as the presence of significant surface inhomogeneities. Figure 4 (right) shows an AFM image of bacterial cellulose grown in a sucrose-containg medium and dried at room temperature. Like in the FD-samples, the pattern of fiber intertwining was rather random, with multiple bends. Nevertheless, direct comparison with the FD-group showed a more uniform surface

Figure 4 AFM images of BC synthesized from sucrose after FD (left) and after RT drying (right). The upper photos demonstrate the roughness of the sample according to the given pseudo-color scales. The pA values represent the photocurrent measured by the optical sensor. The lower row shows 3D-reconstructions of the obtained photos after converting pA units into height/roughness data.
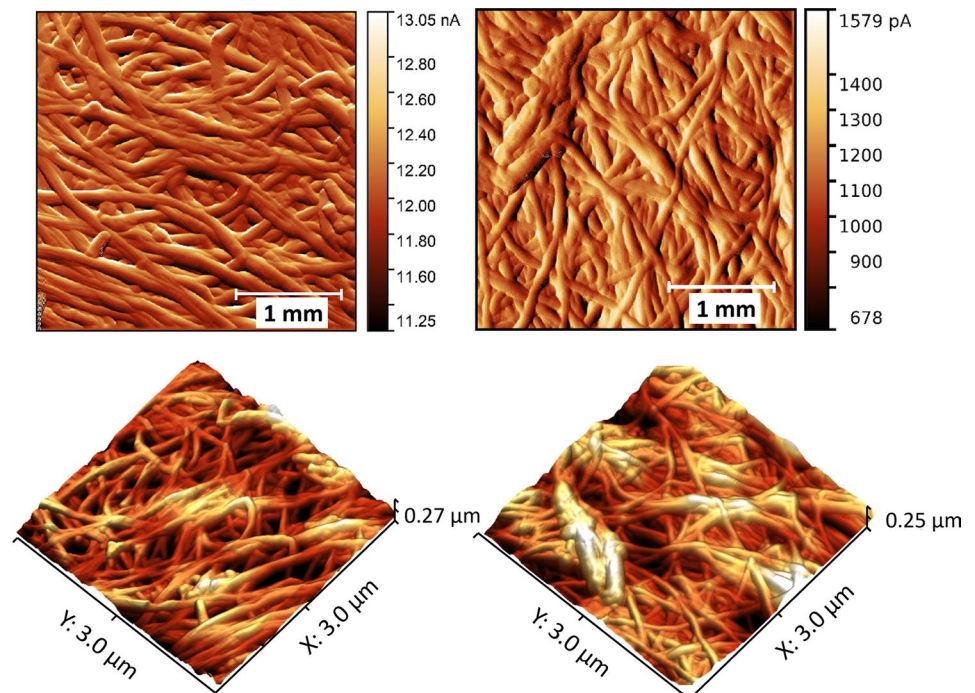
of the RT-samples, with their roughness 68.5 nm. The packing of macrofibers was also denser in comparison with the similar sample obtained by freeze drying and resembled to the glucose-derived BC sample obtained by RT drying.

In both drying methods, the "sucrose group" showed randomly intertwined microfibers with lengths of 13 ± 3 μm. In other words, the microstructure of dried sucrose-derived BC seemingly depended less on the choice of the drying protocol than those of the glucose-derived BC.

As we speculated in our previous article [7], structural differences between films synthesized on glucose and sucrose media may be associated with different responses of microorganisms of the cellulose synthesizing consortium to different carbon sources. Thus, glucose is equally well and quickly metabolized by both yeast organisms and acetic acid bacteria, while sucrose is primarily consumed by yeast, which leads to a delay in the metabolic and biosynthetic response on the part of acetic acid symbionts. Perhaps this asynchrony of the processes of sugar utilization and growth is reflected in the microstructure of the resulting cellulose matrix.

Typical measured diameters of BC fibrils in the FD- and RT-samples were 70 nm and 40 nm, respectively. This is larger than the data published by Zhang et al. but corresponds well to their observation that lyophilization leads to larger average diameters of BC fibers [29]. The same authors reasonably speculated that the larger fiber diameter of the freeze-dried samples may result from the decreased hydrogen bonding between the chains and reduced chain motion due to direct water sublimation.

Further analysis of the images acquired by the AFM method allowed us to conclude that the BC films subjected to freeze-drying were generally characterized by a more branched structure, with a corresponding higher surface roughness (68 ± 10 nm and 81 ± 9 nm for the FD and RT groups, respectively). At the same time, the samples originating from different drying protocols did not differ with respect to the average fibril length (13 ± 3 μm for both the FD and RT groups), and average angle between the fibrils on the material surface (45 ± 15°). A table summarizing the changes in BC microstructure at various levels after RT versus FD drying is presented below (Table 1).

There was a general trend that the samples grown in the sucrose nutrient medium featured multiple bends of macrofibers, while for the samples grown on glucose, straight fibrils were much more typical. Independent from the carbon source used, freeze-dried BC steadily displayed two times higher pore sizes.

Thus, the analysis of the data obtained by AFM confirmed the conclusions made based on SEM images, namely, a big impact of the drying method on the BC structure. This includes less dense packing of fibrils for samples dried by freeze drying and higher porosity of such samples.

Influence of the dehydration method on the BC nanostructure and crystallinity

The effect of different drying protocols can be attributed to the degree of disordering of cellulosic structure, caused by the different arrangements in the angles around β-glycoside linkages and hydrogen bond rearrangement [20]. X-ray diffraction experiments were performed to reveal further parameters of the supramolecular structure of the samples: degree of crystallinity, d-spacing and crystallite sizes. X-ray patterns of BC obtained on glucose-and sucrose-containing media, dried by freeze-drying or at room temperature, are shown in Fig. 5. The obtained experimental data (small pale dots) are shown approximated in the X-ray diffraction pattern built by the Fityk program. Thinner lines of violet, black, and green correspond to different components of the pseudo-Voigt model; the thick orange line represents the superposition all components.

All samples displayed a significant proportion of amorphous cellulose, manifesting itself as high

Table 1 Main AFM- and SEM-derived microstructural parameters of BC films obtained on different substrates and with different drying methods

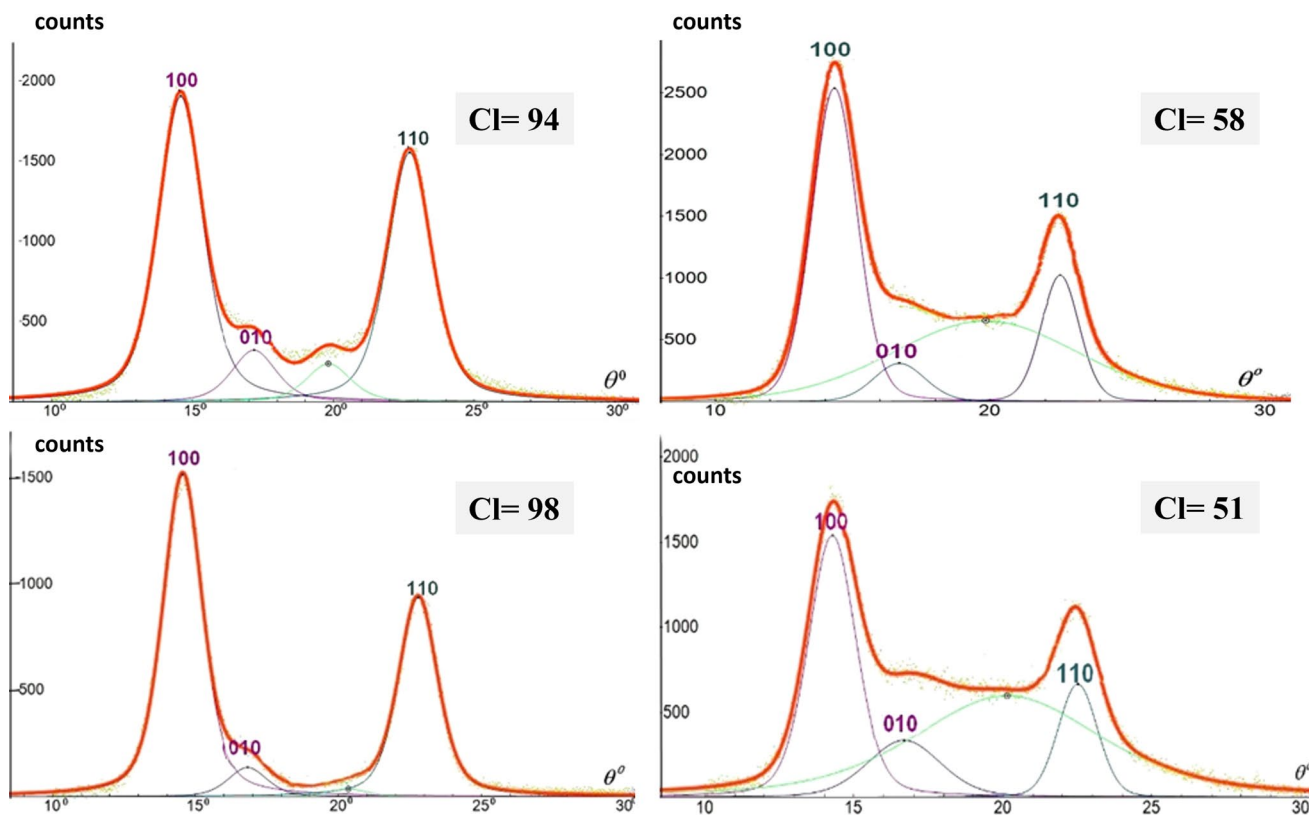| Sample	Average pore diameter, μm	Average roughness over the field 30×30 μm, nm	Average length of fibers, μm	Average diameter of macro fibrils, nm
Glucose FD	0.35 ± 0.07	195 ± 12	50 ± 12	100 ± 15
Glucose RT	0.12 ± 0.04	81 ± 5	30 ± 7	55 ± 6
Sucrose FD	0.20 ± 0.06	68 ± 10	13 ± 3	70 ± 15
Sucrose RT	0.13 ± 0.05	81 ± 9	13 ± 3	40 ± 6

Figure 5 XRD-ray profiles of bacterial cellulose grown on glucose (upper row) and sucrose (lower row), dehydrated by FD (left) and RT drying (right). CI values represent calculated values of corresponding crystallinity indices.

intensity of the reflection (100) compared to the (110). We presume that this occurred due to the disordering in the structure of BC fibrils caused by the drying process. Long-range order in the BC films is partially maintained due to the bonds between water molecules, and the quick process of freeze-drying seemingly preserves this order better. The presence of a pronounced (010) reflection apparently indicates the presence of a noticeable order in the fibrils oriented parallel to the film boundary. As follows from the diffraction patterns measured for the RT-sucrose-samples (Fig. 5, lower row, right), they exhibited especially high content of the amorphous phase.

The obtained integral intensities were further used to calculate the crystallinity index (CI) by the Ruland-Wonk method. This method allows to derive CI from the ratio of the area of the crystalline phase to the total area under the diffraction curve, which includes scattering by the amorphous and crystalline phases. It must be taken into account that the integral intensity of each reflection in the X-ray pattern is proportional to the content of the crystalline phase, while the content of the amorphous component of the cellulose material is proportional to the intensity of diffuse scattering. The values derived of the degree of crystallinity, d-spacing and crystallite sizes are shown in Table 2.

Table 2 Key parameters of supramolecular structure of dehydrated BC samples: degree of crystallinity (CI), d-spacing (d) and crystallite sizes (Cs).

CI, %	Glucose FD			Glucose RT			Sucrose FD			Sucrose RT		
	94			58			98			51		
	(100)	(010)	(110)	(100)	(010)	(110)	(100)	(010)	(110)	(100)	(010)	(110)
d, nm	0.607	0.516	0.391	0.617	0.527	0.395	0.608	0.527	0.390	0.619	0.531	0.395
Cs, nm	4.56	4.62	4.79	4.42	3.94	5.55	5.29	5.35	5.56	4.56	3.09	5.76

As follows from the calculated CI values, the choice of the BC dehydration method appears to be critical for the crystallinity degree of the dried material. For both glucose- and sucrose-grown BC films, the freeze-drying caused significantly higher crystallinity indices (94 and 98, respectively, as compared to the RT samples (58 and 51, respectively). This agrees with the data reported previously by Zhang et al. but is significantly more pronounced compared to their results [29]. The reasons for this (minor) deviation might be differences in bacterial strains and laboratory protocols used for BC-production as well as in the settings of the applied drying protocols.

The calculated values of the distance between atomic planes (d) suggested an increase in this parameter in all directions in the RT samples. A possible reason for this is that the initial ordering of glucan chains, present in the native (raw) cellulose is better preserved during freeze-drying. This creates internal tension supported by the packing of crystallites, which fraction is the largest in these samples (an additional indicator here is a high degree of crystallinity). RT-drying seemingly lead to disordering of glucan chains occurs, accompanied by a decrease in the degree of crystallinity and in the interplanar distance, as well as by a decrease in the size of crystallites.

The calculated crystallinity parameters presented in Table 2 are consistent with our AFM data. The largest crystallite sizes (reaching 5.56 nm) were characteristic for the FD samples. This indicates better preservation of originally ordered regions in the BC molecular structure after freeze drying.

In accordance with the modern understanding of the amorphous-crystalline structure of cellulose, fragments of ordered (crystalline) and amorphous phases spatially alternate in the cellulose material [11]. Since the three-dimensional long-range order is maintained by intermolecular orientational interactions (e.g., van der Waals forces), it becomes weaker with increasing thickness of the gel film. However, the high proportion of the amorphous phase in the RT samples implies the distinctive role of water in maintaining of this order. The freeze-drying seemed to preserve the order existing in the native samples, probably due to the restricting of fibril mobility upon quick low-temperature dehydration. In the RT-samples, fibrils tended to aggregate, which lead to an increase in the proportion of the amorphous phase and was manifested in an increase in the number of broadened fibrils segments visible under AFM.

As we showed in our previous work [7], on the substrates with sucrose the rate of BC formation was lower than on those containing glucose. Due to the lower rate of BC synthesis, the crystallite sizes in BC on sucrose are larger, since there was more time for crystal bond formation. The same factor can be responsible for the formation of a more complex, "chaotic" arrangement of BC fibers, revealed by AFM in the sucrose-derived films.

Conclusions

Many current and future applications of BC materials are based on their distinct morphology, physico-chemical, and biological properties. One of the factors critically responsible for BC mechanical strength, water absorption capacity, is the character of fibers intertwining, defining the overall matrix and surface microstructure.

Analysis of the spatial structure of cellulose fiber in a native BC gel film containing only 1.5–2% dry matter is a complex technical task. In this regard, structural studies using various methods are carried out typically only for pre-dried samples. However, our study, like several studies done before, indicates that, depending on the drying method, the structure formed differs significantly both at the macro level and at the level of individual fibrils.

Our study showed that BC samples treated by freeze-drying were generally characterized by a more branched structure, higher surface roughness, greater porosity, and significantly higher crystallinity degree. These main findings are principally and mostly in agreement with those published during the last 20 years, but for some aspects, our study provided significantly different magnitudes or even directions of the observed effects.

As emphasized by Clasen et al. [5], the drying method is just one of the factors defining the BC structure; therefore, its role should be analyzed in a broader methodological context. In contrast to many previous studies, we examined not only two different drying protocols but also their impact on two different raw bacterial cellulose materials and found that the origin of the BC may also influence the extent and character of its changes caused by a chosen drying method.

In general, the analysis of data obtained using SEM, AFM and XRD shows an increase in the ordering of the fibrillar structure of the samples by using the

freeze-drying method. On the contrary, room temperature drying leads to filling the interfibrillar space with an amorphous phase. As an additional influencing factor, samples grown in a sucrose nutrient medium were always characterized by the thinning of microfibrils with their more chaotic packing and a greater degree of disorder in their spatial orientation.

We conclude that both the structure of the wet BC pellet and the choice of drying method can strongly affect the properties of the dried BC materials and should be both taken into consideration. For example, the RT drying process of BC might be preferential in the applications requiring better barrier properties requirement, whereas FD-method appears to be advantageous in the production of BC materials featuring high porosity or controlled swelling behavior.

Acknowledgements

Author contributions

ID—wrote and drafted the manuscript, including presentation and visualization of the results; NA—performed literature survey, contributed to the interpretation of all data and to drafting of the manuscript; NP—is the creator of the manuscript concept. She personally collected and analyzed all microbiological data and performed atomic force microscopy; ER—performed FE-SEM, AFM and XRD. He analyzed and interpreted the obtained diffraction data. All authors approved the final version of the manuscript.

Funding

Declarations

References

[1] Balzar D, Ledbetter H (1993) Voigt-function modeling in Fourier analysis of size- and strain-broadened X-ray diffraction peaks. J Appl Crystallogr 26(1):97–103

[2] Bordun I, Chwastek K, Całus D, Chabecki P, Ivashchyshyn F, Kohut Z, Borysiuk A, Kulyk Y (2021) Comparison of structure and magnetic properties of Ni/C composites synthesized from wheat straw by different methods. Appl Sci 11(21):10031

[3] Cheng K-C, Catchmark JM, Demirci A (2009) Effect of different additives on bacterial cellulose production by *Acetobacter xylinum* and analysis of material property. Cellulose 16(6):1033–1045

[4] Chernigova SV, Zubkova NV, Chernigov YV, Pogorelova NA (2019) Morphological changes in the tissue structures after thermal burns on the background of using dermarm wound dressing. La Prensa Méd Argent 105(9):521–254

[5] Clasen C, Sultanova B, Wilhelms T, Heisig P, Kulicke W-M (2006) Effects of different drying processes on the

material properties of bacterial cellulose membranes. Macromol Symp 244(1):48–58

[6] David WIF (1986) Powder diffraction peak shapes. Parameterization of the pseudo-Voigt as a Voigt function. J Appl Crystallogr 19(1):63–64

[7] Digel I, Akimbekov N, Rogachev E, Pogorelova N (2023) Bacterial cellulose produced by *Medusomyces gisevii* on glucose and sucrose: biosynthesis and structural properties. Cellulose 30(18):11439–11453

[8] Domskiene J, Sederaviciute F, Simonaityte J (2019) Kombucha bacterial cellulose for sustainable fashion. IJCST 31(5):644–652

[9] Fang L, Catchmark JM (2014) Structure characterization of native cellulose during dehydration and rehydration. Cellulose 21(6):3951–3963

[10] French AD (2014) Idealized powder diffraction patterns for cellulose polymorphs. Cellulose 21(2):885–896

[11] Hajlaoui O, Khiari R, Ajili L, Batis N, Bergaoui L (2020) Design and characterization of type I cellulose-polyaniline composites from various cellulose sources: a comparative study. Chemistry Afr 3(3):783–792

[12] Illa MP, Sharma CS, Khandelwal M (2019) Tuning the physiochemical properties of bacterial cellulose: effect of drying conditions. J Mater Sci 54(18):12024–12035

[13] Jarrell J, Cal T, Bennett JW (2000) The Kombucha consortia of yeasts and bacteria. Mycologist 14(4):166–170

[14] Jayabalan R, Malbaša RV, Lončar ES, Vitas JS, Sathishkumar M (2014) A review on kombucha tea-microbiology, composition, fermentation, beneficial effects, toxicity, and tea fungus. Compr Rev Food Sci Food Saf 13(4):538–550

[15] Lahiri D, Nag M, Dutta B, Dey A, Sarkar T, Pati S, Edinur HA, Abdul Kari Z, Mohd Noor NH, Ray RR (2021) Bacterial cellulose: production, characterization, and application as antimicrobial agent. Int J Mol Sci 22(23):12984

[16] Madihally SV, Matthew HW (1999) Porous chitosan scaffolds for tissue engineering. Biomaterials 20(12):1133–1142

[17] Mohamad S, Abdullah LC, Jamari SS, Al Edrus SSO, Aung MM, Mohamad SFS (2022) Influence of drying method on the crystal structure and thermal property of oil palm frond juice-based bacterial cellulose. J Mater Sci 57(2):1462–1473

[18] Nečas D, Klapetek P (2012) Gwyddion: an open-source software for SPM data analysis. Open Phys 10(1):99

[19] Pogorelova N, Rogachev E, Digel I, Chernigova S, Nardin D (2020) Bacterial cellulose nanocomposites: morphology and mechanical properties. Materials 13(12):2849

[20] Proniewicz LM, Paluszkiewicz C, Wesełucha-Birczyńska A, Barański A, Dutka D (2002) FT-IR and FT-Raman study of hydrothermally degraded groundwood containing paper. J Mol Struct 614(1–3):345–353

[21] Reiniati I, Hrymak AN, Margaritis A (2017) Recent developments in the production and applications of bacterial cellulose fibers and nanocrystals. Crit Rev Biotechnol 37(4):510–524

[22] Ross P, Mayer R, Benziman M (1991) Cellulose biosynthesis and function in bacteria. Microbiol Rev 55(1):35–58

[23] Rosyida VT, Indrianingsih AW, Hayati SN, Apriyana W (2020) The effect of different drying temperature on crystallinity and morphology structure of bacterial cellulose. IOP Conf Ser: Earth Environ Sci 462(1):12050

[24] Seifert M, Hesse S, Kabrelian V, Klemm D (2004) Controlling the water content of never dried and reswollen bacterial cellulose by the addition of water-soluble polymers to the culture medium. J Polym Sci A Polym Chem 42(3):463–470

[25] Sumadiyasa M, Manuaba IBS (2018) Determining crystallite size using Scherrer formula, Williamson-Hull plot, and particle size with SEM. Bul Fis 19(1):28–35

[26] Thongsomboon W, Serra DO, Possling A, Hadjineophytou C, Hengge R, Cegelski L (2018) Phosphoethanolamine cellulose: a naturally produced chemically modified cellulose. Science 359(6373):334–338

[27] Vasconcellos V, Farinas C (2018) The effect of the drying process on the properties of bacterial cellulose films from *Gluconacetobacter hansenii*. Chem Eng Trans 64:145–150

[28] Wojdyr M (2010) Fityk : a general-purpose peak fitting program. J Appl Crystallogr 43(5):1126–1128

[29] Zhang CJ, Wang L, Zhao JC, Zhu P (2011) Effect of drying methods on structure and mechanical properties of bacterial cellulose films. AMR 239–242:2667–2670